Featured in Physics

Collective Relaxation Dynamics in a Three-Dimensional Lattice Glass Model

Yoshihiko Nishikawa[1,*] and Ludovic Berthier[2,3]
[1]Graduate School of Information Sciences, Tohoku University, Sendai 980-8579, Japan
[2]Laboratoire Charles Coulomb (L2C), Université de Montpellier, CNRS, 34095 Montpellier, France
[3]Yusuf Hamied Department of Chemistry, University of Cambridge, Lensfield Road, Cambridge CB2 1EW, United Kingdom

(Received 16 August 2023; accepted 20 December 2023; published 7 February 2024)

We numerically elucidate the microscopic mechanisms controlling the relaxation dynamics of a three-dimensional lattice glass model that has static properties compatible with the approach to a random first-order transition. At low temperatures, the relaxation is triggered by a small population of particles with low-energy barriers forming mobile clusters. These emerging quasiparticles act as facilitating defects responsible for the spatially heterogeneous dynamics of the system, whose characteristic length scales remain strongly coupled to thermodynamic fluctuations. We compare our findings both with existing theoretical models and atomistic simulations of glass formers.

DOI: 10.1103/PhysRevLett.132.067101

The glass transition of supercooled liquids is characterized by a drastic dynamical slowing down, with timescales that increase much faster than the Arrhenius law in fragile glass formers [1,2]. These dynamics become increasingly spatially heterogeneous upon approaching the glass transition [3,4], in a manner revealed by four-point dynamic susceptibilities and correlation functions [4–7]. Over the last decade, massive efforts were also deployed to establish and characterize the growth of relevant thermodynamic fluctuations and static correlation length scales accompanying this slowing down [8–11], with results compatible with an approach to a random first-order transition (RFOT) [12–16].

The central open question that remains, then, concerns the existence of a causal link between static and dynamic fluctuations, to go beyond known correlations [17]. While RFOT theory suggests that static fluctuations directly control the evolution of dynamic heterogeneity and explain the slowing down of the dynamics [18–20], alternative approaches use local energy barriers and dynamic facilitation [21–25], making no reference to the underlying complex free energy landscape.

Experimental measurements do not easily discriminate these views [26], and original strategies are needed [27]. Recent developments in computational studies of atomistic glass formers [28] helped reveal the importance of dynamic facilitation at very low temperatures [29–32], strengthening earlier results [24,33]. The reported decoupling between static and dynamic length scales [32,34] weakens the idea that statics fully controls dynamics, as does the observation that local Monte Carlo algorithms strongly impact the equilibrium dynamics [35]. While RFOT theory accounts for all these observations [20,36,37], the current situation is confused.

Simplified lattice models with minimal (but not too minimal) ingredients are ideally suited to clarify these questions [2]. Kinetically constrained lattice glass models have no complex thermodynamics but display dynamic heterogeneity stemming instead from dynamic facilitation and kinetic constraints [38–42]. Interacting plaquette spin models form another class, in which similar kinetic constraints emerge from interacting degrees of freedom [43–45]. Finally, lattice glass models with frustrated interactions also exist [46–50]. Differently from the other two families, they display, just like atomistic models, a random first-order transition in the mean-field limit. They are therefore ideal candidates to study the interplay between static and dynamic fluctuations in finite dimensions. This is the central motivation for our work.

Recently [51], a lattice glass model with good glass-forming ability in $d = 3$ was numerically shown to display thermodynamic fluctuations consistent with both RFOT theory and finite-d glass formers. Here, we study its dynamics to shed light on how structural relaxation occurs in a many-body particle system approaching a RFOT. We find that the dynamics becomes glassy and spatially heterogeneous, with a strong coupling between static and dynamic fluctuations. However, structural relaxation is triggered by emerging quasiparticles composed of localized clusters of particles with low-energy barriers, which gradually relax the correlated slow regions in a manner reminiscent of dynamic facilitation. While statics plays a role in the dynamics, this differs strongly from the predictions of RFOT theory.

We study a binary mixture of particles [51] on a periodic cubic lattice of linear dimension L and Hamiltonian

$$H = \sum_i \left(\sum_j \delta(|\boldsymbol{r}_i - \boldsymbol{r}_j|, 1) - \ell_{\sigma_i} \right)^2, \tag{1}$$

with $\delta(\cdot,\cdot)$ the Kronecker delta, $\boldsymbol{r}_i$ the position of particle i taking values $r_{i,\alpha} = 1, 2, \ldots L$ ($\alpha = x, y, z$), and $\sigma_i \in \{1, 2\}$

specifying the particle type. Each particle type has a preferred number of neighbors, ℓ_σ, and quadratic deviations from this number provide the local energy cost; see SM [52]. We set $\ell_1 = 3$ and $\ell_2 = 5$, fix the density to $\phi = N/L^3 = 0.75$, where N is the number of particles, and the concentrations $\rho_1 = N_1/N = 0.4$ and $\rho_2 = N_2/N = 0.6$ [51]. We use $L = 20$, apart from the temperature $T = 0.26$, where we set $L = 10$ as the simulations take much longer to converge.

To obtain equilibrium configuration of the system defined by Eq. (1) we use a nonlocal swap dynamics, where two lattice sites with different occupation numbers or particle types are randomly chosen and swapped with Metropolis probability. To study the physical dynamics, we restrict the above rule to pairs of nearest neighbors [51]. This local dynamics allows us to explore structural relaxation down to $T \approx 0.3$, while Ref. [51] locates the putative Kauzmann transition near $T \approx 0.24$. At $T = 0.3$, the nonlocal swap provides a comfortable speedup of about 10^3, allowing us to explore the equilibrium dynamics of the model at temperature where the physical dynamics is extremely slow. The unit time represents L^3 attempted moves.

The structural relaxation of the system can be followed using the collective overlap

$$\langle Q(t)\rangle = \frac{1}{1-Q_0}\left\langle \frac{1}{N}\sum_i q_i(t) - Q_0 \right\rangle. \tag{2}$$

In this expression the local overlap $q_i(t)$ remains 1 only when the site occupied by particle i at time 0 is again occupied by any particle of the same type at time t later, where $q_i(t) = \sum_j \delta(\boldsymbol{r}_i(0), \boldsymbol{r}_j(t))\delta(\sigma_i(0), \sigma_j(t))$ and $Q_0 = \phi(\rho_1^2 + \rho_2^2)$. The brackets $\langle\cdot\rangle$ stand for an average over initial equilibrium configurations. The collective overlap in Eq. (2) is the lattice analog of the overlap defined for particle systems [10]. It is normalized to decay from 1 to 0 when the structure at $t = 0$ has fully relaxed. Numerical results are shown in Fig. 1(a). At high temperatures $T \gg 1$, the system rapidly decorrelates. When $T \lesssim 0.55$, $\langle Q(t)\rangle$ starts to have a plateau [see enlargement in Fig. 1(b)] and the corresponding relaxation time τ_α departs from an Arrhenius behavior; see Fig. 1(c).

With decreasing T further, the dynamics keeps slowing down, and at very low temperatures $T \lesssim 0.325$, a more complex short time dynamics emerges. This is better appreciated in the Fourier relaxation spectrum [56]

$$\chi''(\omega) = \int d\log\tau \frac{d\langle Q(\tau)\rangle}{d\log(\tau)} \frac{\omega\tau}{1+(\omega\tau)^2}, \tag{3}$$

as shown in Fig. 1(d) (see details in SM [52]). This representation clearly reveals additional relaxation processes taking place at intermediate frequencies between the microscopic peak and the main peak corresponding to the structural relaxation, in qualitative agreement with recent observations in particle models [30,31].

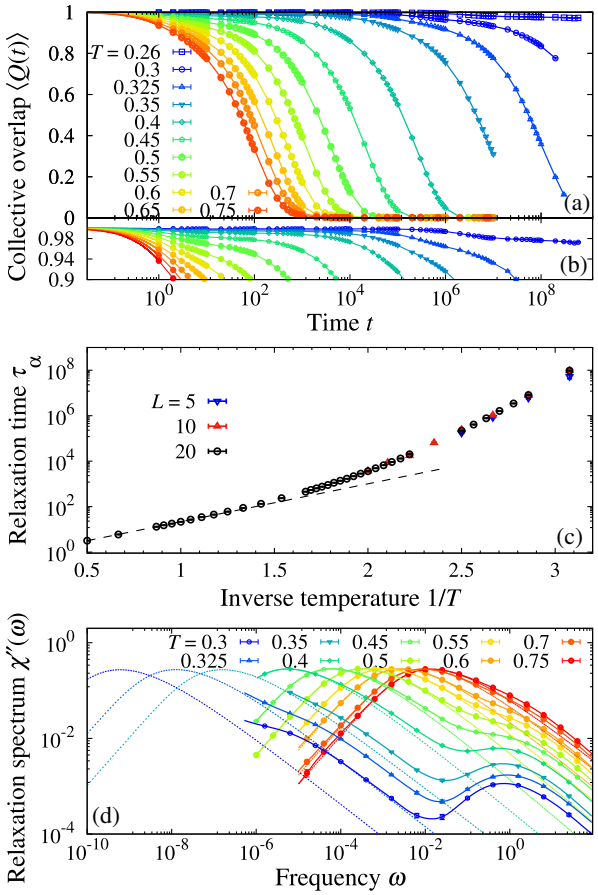

FIG. 1. (a),(b) Temperature evolution of the collective overlap $\langle Q(t)\rangle$. (c) Arrhenius plot of the relaxation time τ_α; the broken line is an Arrhenius fit valid at high temperatures. (d) Relaxation spectrum from Eq. (3); dashed curves represent the spectrum corresponding to the final stretched exponential decay of the overlap.

We turn to the mean-squared displacement (MSD)

$$\langle \Delta^2(t)\rangle = \left\langle \frac{1}{N}\sum_i |\boldsymbol{r}_i(t) - \boldsymbol{r}_i(0)|^2 \right\rangle, \tag{4}$$

to understand how particle motion leads to structural relaxation; see Fig. 2(a). We find, as usual, that the MSD only becomes diffusive at long enough times, after a transient plateau that becomes longer at lower temperatures and a decreasing diffusion constant. However, the MSD slows down much less than the overlap. For instance, at the lowest temperature $T = 0.26$ and at $t = 3 \times 10^8$, $\langle Q(t)\rangle \simeq 0.98$ while $\langle \Delta^2(t)\rangle \simeq 10^2$. It is *a priori* surprising that such large particle displacements lead to so little relaxation in the structure.

To better understand this finding, we determine the corresponding van Hove distribution

$$P_t(\Delta x) = \left\langle \frac{1}{3N}\sum_{i,\alpha} \delta\{\Delta x - [r_{i,\alpha}(t) - r_{i,\alpha}(0)]\} \right\rangle; \tag{5}$$

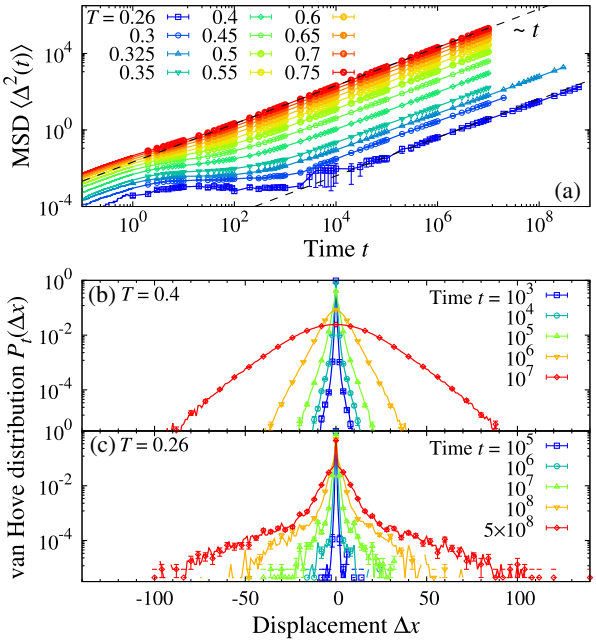

FIG. 2. (a) Time dependence of the MSD; diffusive behavior is indicated with dashed lines. The van Hove distribution functions at (b) $T = 0.4$ where $\tau_\alpha \simeq 2 \times 10^5$ and (c) $T = 0.26$ where $\tau_\alpha \gg 10^{10}$.

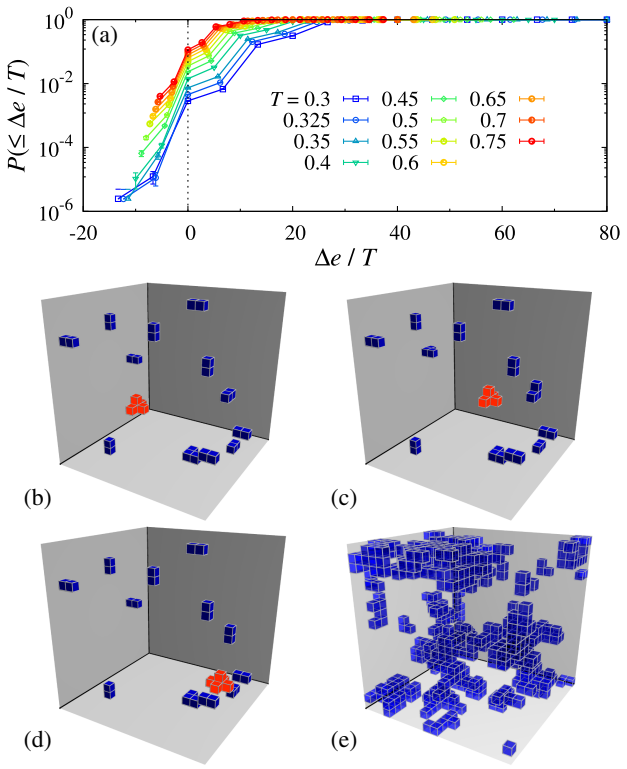

FIG. 3. (a) Cumulative distribution of local energy barriers. The vertical line indicates $\Delta e = 0$. (b)–(d) Snapshots showing lattice sites with $\Delta e \leq 0$ at $T = 0.3$ at three different times. The time intervals between (b) and (c) and between (c) and (d) are 50 and 350, respectively. Sites highlighted in red belong to a quasiparticle moving rapidly. (e) Lattice sites with states that differ between times 0 and 7×10^4, showing the superposition of multiple quasiparticle paths.

see Figs. 2(b) and 2(c). At high temperatures, the particle dynamics is diffusive and $P_t(\Delta x)$ very close to a Gaussian at any time. In contrast, $P_t(\Delta x)$ is non-Gaussian at short times with nearly exponential tails [57] when decreasing temperature, and only becomes Gaussian when $t \gg \tau_\alpha$; see $T = 0.4$ in Fig. 2(b). At very low temperature, e.g., $T = 0.26$ in Fig. 2(c), $P_t(\Delta x)$ develops extremely extended tails coexisting with a large peak at $\Delta x = 0$. This peak corresponds to a large fraction of particles that have not moved at all since $t = 0$, coexisting with a population of particles that have covered distances up to tens of lattice sites. Clearly, dynamics is highly heterogeneous, and different particles can exhibit different behavior. Also, the large decoupling between the overlap and the MSD arises because a small fraction of particles travels large distances while many others have not yet moved.

The emergence of a small population of fast moving particles in an otherwise nearly frozen backbone is unexpected as it is not directly included in the Hamiltonian in Eq. (1), contrary to kinetically constrained models. To understand this feature, we measure for lattice site i in an equilibrium configuration a local energy barrier, Δe_i, defined as the minimum energy cost to swap with one of its nearest neighbors. Such analysis is not possible in off-lattice models, but is very easy here. We show in Fig. 3(a) the cumulative probability distribution of $\Delta e/T$. Lattice sites with $\Delta e/T \geq 10$, for instance, are only swapped with probability $\leq 10^{-4}$. At high temperature, a large fraction of lattice sites have $\Delta e/T \leq 0$ and can move with no rejection. With decreasing temperature, local energy barriers become very large. At $T = 0.3$, a majority of sites have $\Delta e/T \geq 26$, yielding a local timescale $\geq 10^{11}$. Strikingly, however, a fraction of about 0.1% of the lattice sites remains totally free to swap.

In Figs. 3(b)–3(d), we show the lattice sites with $\Delta e \leq 0$ at $T = 0.3$. A significant fraction of these are dimers and trimers, which result in reversible local particle exchanges. More rarely, we observe a larger cluster, as highlighted in red. Our visualizations indicate that these localized clusters can move very rapidly throughout the system. In the example of Fig. 3, the cluster travels more than $L/2$ over about 400 time steps. The identity of the particles that belong to the cluster also changes rapidly. Therefore, these fast moving localized clusters are *emerging quasiparticles* that can move large distances. Particles advected by clusters are responsible for the extended tails in the van Hove distributions.

After many quasiparticles have been observed, the sites that have relaxed are not homogeneously distributed, as shown in Fig. 3(e). This suggests the existence of specific paths along which the motion of quasiparticles occurs preferentially. As a corollary, there exist large compact

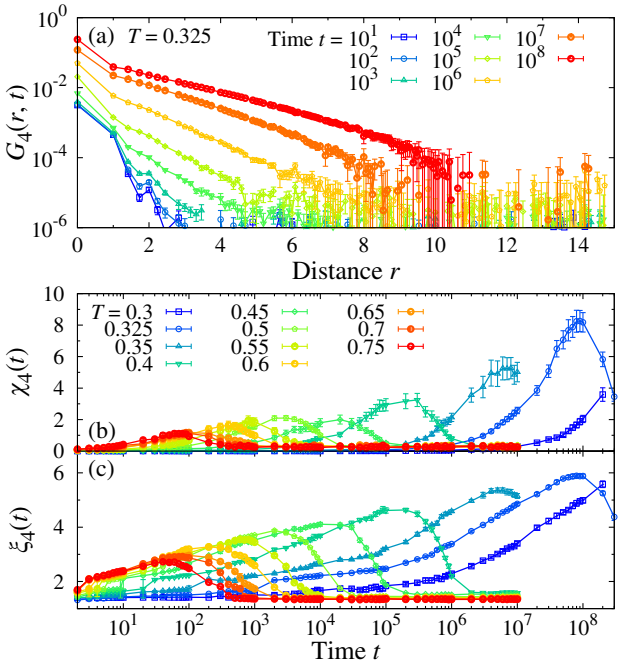

FIG. 4. (a) Four-point correlation function $G_4(r,t)$ at $T = 0.325$ where $\tau_\alpha \approx 10^8$. (b) Dynamical susceptibility $\chi_4(t)$ and (c) dynamical length scale $\xi_4(t)$ demonstrating increasing dynamic heterogeneity.

domains in which fast motion cannot occur and can only relax by the repeated motion of many quasiparticles at their boundaries. This represents, for the lattice glass model under study, the analog of the dynamic facilitation reported for off-lattice simulations [24,32].

To describe more quantitatively the emerging dynamic heterogeneity, we measure the four-point correlation function $G_4(r,t)$, defined as

$$G_4(r,t) = \frac{1}{4\pi r^2}\left\langle \frac{1}{N}\sum_{i,j}\delta q_i(t)\delta q_j(t)\delta(r - |\boldsymbol{r}_i - \boldsymbol{r}_j|)\right\rangle, \quad (6)$$

with $\delta q_i(t) = q_i(t) - \sum_j \langle q_j(t)\rangle/N$ the local fluctuation of the overlap. We extract the dynamic length scale $\xi_4(t)$ using the definition $G_4(\xi_4,t)/G_4(0,t) = 10^{-2}$, as well as the dynamical susceptibility $\chi_4(t) = \int dr 4\pi r^2 G_4(r,t)$. At high temperatures, $G_4(r,t)$ decays rapidly over a few lattice sites even near τ_α, showing that relaxation is purely local. Spatial correlations revealed by a much slower decay in $G_4(r,t)$ appear at lower temperatures; see Fig. 4(a) for $T = 0.325$ where ξ_4 grows up to $\xi_4 \approx 6$ near $\tau_\alpha \approx 10^8$. This evolution is observed for both ξ_4 and χ_4, whose time dependencies are shown in Fig. 4. These data are familiar [6], with a slow growth for $t \ll \tau_\alpha$ followed by a maximum near τ_α. Interestingly, at very low temperatures, the slow growth of ξ_4 toward its peak is compatible with a power law, $\xi_4 \sim t^{1/z}$, with a small exponent $1/z \approx 0.15$, in line with recent off-lattice findings [32].

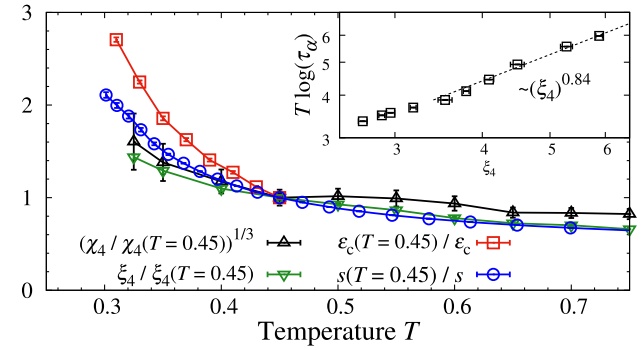

FIG. 5. Evolution of two estimates of a dynamic length scale, $(\chi_4)^{1/3}$ and ξ_4, and of two estimates of a static correlation length scale $1/s(T)$ and $1/\varepsilon_c(T)$. Each quantity is normalized by its value at $T = 0.45$. Inset shows $T\log(\tau_\alpha)$ as a function of ξ_4; the dashed line is a fit to $\log(\tau_\alpha) \sim \xi_4^\psi/T$ with $\psi = 0.84$.

We collect all relevant length scales in Fig. 5 where we show both ξ_4 and χ_4 measured at their maximum near τ_α. Our data indicate that the simple relation $\chi_4 \sim \xi_4^3$ holds (not shown), confirming that slow domains have a compact geometry and thus we report the quantity $\chi_4^{1/3}$ in Fig. 5. We normalize these quantities by their values at temperature $T = 0.45$, below which important thermodynamic quantities have been determined before [51].

Two estimates of the configurational entropy [53] were measured. First, the total entropy $s(T)$ itself was measured using thermodynamic integration. It should be close to the configurational entropy since vibrational contributions are negligible on the lattice. Second, the inverse of the critical coupling field ε_c [51] in the Franz-Parisi scheme [54] also represents a solid estimate of the configurational entropy [55], which is itself inversely proportional to the point-to-set correlation length scale quantifying static correlations [18,19,53] (see SM [52] for a review of these connections). These two indirect estimates of a static length scale are included in Fig. 5, also rescaled at $T = 0.45$. They appear to grow at least as significantly (if not more strongly) than dynamic length scales. The coupling between static and dynamic length scales is therefore stronger here than in atomistic models [10,32,34,58]. This finding encourages us to directly test the relation between timescales and length scales predicted in RFOT theory; see Fig. 5, where the relation $\log\tau_\alpha \sim \xi_4^\psi/T$ with $\psi \approx 0.84$ is followed by the data. While a larger exponent ψ (between $d/2$ and d) is expected from cooperative relaxation events, it is not surprising that a lower apparent value is found here, as dynamic facilitation via mobile quasiparticles provides more efficient dynamic pathways. This result indicates that the RFOT theory picture of cooperative activated dynamics is not dominant for the studied model. Interestingly, values $\psi < 1$ were also inferred from analysis of experimental data [59,60] and numerically [9,61].

In conclusion, our results establish that, differently from all other classes of lattice models for glassy dynamics, the 3D lattice glass model studied here displays thermodynamic and dynamic properties that compare favorably with atomistic glass formers, with growing static point-to-set and four-point dynamic length scales. While static and dynamic fluctuations appear to be strongly coupled, the relaxation dynamics is nevertheless different from the RFOT theory description invoking cooperative relaxation events. Instead, while the system genuinely approaches a random first-order transition, it also leaves behind a small population of weakly constrained particles forming emergent quasiparticles whose fast propagation slowly relaxes the entire system eventually at large times. These quasiparticles thus resemble the dynamic defects postulated in kinetically constrained models, or those emerging from the specific interactions of plaquette models. They also lead to signatures at intermediate timescales that are reminiscent of recent findings in atomistic models [30,32].

While details of the emergent quasiparticles and dynamical defects may be specific to our model, the physical picture emerging from our study appears generic. It is consistent with the recent body of results regarding glassy dynamics at very low temperatures and it supports the generic conclusion that cooperative events from statically correlated domains are preempted by faster relaxation events involving localized regions acting as facilitating defects [31,32,62]. Our results provide a unified picture for glassy dynamics near the glass transition where facilitated dynamics takes place near localized regions, whose temperature evolution is strongly connected to emerging static correlations. We hope that future studies will confirm the validity of these conclusions across a broader range of models (including molecular systems) and spatial dimensions, and study the fate of models even closer to the putative ideal glass transition where cooperative events could finally become dynamically relevant.

We thank P. Charbonneau, A. Ikeda, H. Ikeda, J. Takahashi, H. Yoshino, and F. Zamponi for useful discussions. Y. N. acknowledges support from JSPS KAKENHI (Grant No. 22K13968), L. B.'s work is supported by a grant from the Simons Foundation (No. 454933).

*Present address: Department of Physics, Kitasato University, Sagamihara 252-0373, Kanagawa, Japan.

[1] P. G. Debenedetti and F. H. Stillinger, Supercooled liquids and the glass transition, Nature (London) **410**, 259 (2001).
[2] L. Berthier and G. Biroli, Theoretical perspective on the glass transition and amorphous materials, Rev. Mod. Phys. **83**, 587 (2011).
[3] M. D. Ediger, Spatially heterogeneous dynamics in supercooled liquids, Annu. Rev. Phys. Chem. **51**, 99 (2000).
[4] L. Berthier, G. Biroli, J.-P. Bouchaud, L. Cipelletti, and W. van Saarloos, *Dynamical Heterogeneities in Glasses, Colloids, and Granular Media* (Oxford University Press, New York, 2011).
[5] N. Lačević, F. W. Starr, T. B. Schrøder, and S. C. Glotzer, Spatially heterogeneous dynamics investigated via a time-dependent four-point density correlation function, J. Chem. Phys. **119**, 7372 (2003).
[6] C. Toninelli, M. Wyart, L. Berthier, G. Biroli, and J.-P. Bouchaud, Dynamical susceptibility of glass formers: Contrasting the predictions of theoretical scenarios, Phys. Rev. E **71**, 041505 (2005).
[7] S. Karmakar, C. Dasgupta, and S. Sastry, Growing length scales and their relation to timescales in glass-forming liquids, Annu. Rev. Condens. Matter Phys. **5**, 255 (2014).
[8] G. Biroli, J.-P. Bouchaud, A. Cavagna, T. S. Grigera, and P. Verrocchio, Thermodynamic signature of growing amorphous order in glass-forming liquids, Nat. Phys. **4**, 771 (2008).
[9] S. Karmakar, C. Dasgupta, and S. Sastry, Growing length and time scales in glass-forming liquids, Proc. Natl. Acad. Sci. U.S.A. **106**, 3675 (2009).
[10] W. Kob, S. Roldán-Vargas, and L. Berthier, Non-monotonic temperature evolution of dynamic correlations in glass-forming liquids, Nat. Phys. **8**, 164 (2012).
[11] L. Berthier, Overlap fluctuations in glass-forming liquids, Phys. Rev. E **88**, 022313 (2013).
[12] L. Berthier, P. Charbonneau, D. Coslovich, A. Ninarello, M. Ozawa, and S. Yaida, Configurational entropy measurements in extremely supercooled liquids that break the glass ceiling, Proc. Natl. Acad. Sci. U.S.A. **114**, 11356 (2017).
[13] L. Berthier, P. Charbonneau, A. Ninarello, M. Ozawa, and S. Yaida, Zero-temperature glass transition in two dimensions, Nat. Commun. **10**, 1508 (2019).
[14] B. Guiselin, L. Berthier, and G. Tarjus, Random-field Ising model criticality in a glass-forming liquid, Phys. Rev. E **102**, 042129 (2020).
[15] B. Guiselin, L. Berthier, and G. Tarjus, Statistical mechanics of coupled supercooled liquids in finite dimensions, SciPost Phys. **12**, 091 (2022).
[16] B. Guiselin, G. Tarjus, and L. Berthier, Is glass a state of matter?, Phys. Chem. Glasses **63**, 136 (2022).
[17] R. Richert and C. A. Angell, Dynamics of glass-forming liquids. V. On the link between molecular dynamics and configurational entropy, J. Chem. Phys. **108**, 9016 (1998).
[18] T. R. Kirkpatrick, D. Thirumalai, and P. G. Wolynes, Scaling concepts for the dynamics of viscous liquids near an ideal glassy state, Phys. Rev. A **40**, 1045 (1989).
[19] J.-P. Bouchaud and G. Biroli, On the Adam-Gibbs-Kirkpatrick-Thirumalai-Wolynes scenario for the viscosity increase in glasses, J. Chem. Phys. **121**, 7347 (2004).
[20] G. Biroli and J.-P. Bouchaud, The RFOT theory of glasses: Recent progress and open issues, C.R. Phys. **24**, 1 (2023).
[21] J. P. Garrahan and D. Chandler, Geometrical explanation and scaling of dynamical heterogeneities in glass forming systems, Phys. Rev. Lett. **89**, 035704 (2002).
[22] J. P. Garrahan and D. Chandler, Coarse-grained microscopic model of glass formers, Proc. Natl. Acad. Sci. U.S.A. **100**, 9710 (2003).

[23] D. Chandler and J. P. Garrahan, Dynamics on the way to forming glass: Bubbles in space-time, Annu. Rev. Phys. Chem. **61**, 191 (2010).
[24] A. S. Keys, L. O. Hedges, J. P. Garrahan, S. C. Glotzer, and D. Chandler, Excitations are localized and relaxation is hierarchical in glass-forming liquids, Phys. Rev. X **1**, 021013 (2011).
[25] J. C. Dyre, Colloquium: The glass transition and elastic models of glass-forming liquids, Rev. Mod. Phys. **78**, 953 (2006).
[26] S. Albert, T. Bauer, M. Michl, G. Biroli, J.-P. Bouchaud, A. Loidl, P. Lunkenheimer, R. Tourbot, C. Wiertel-Gasquet, and F. Ladieu, Fifth-order susceptibility unveils growth of thermodynamic amorphous order in glass-formers, Science **352**, 1308 (2016).
[27] L. Berthier, Self-induced heterogeneity in deeply supercooled liquids, Phys. Rev. Lett. **127**, 088002 (2021).
[28] L. Berthier and D. R. Reichman, Modern computational studies of the glass transition, Nat. Rev. Phys. **5**, 102 (2023).
[29] R. N. Chacko, F. P. Landes, G. Biroli, O. Dauchot, A. J. Liu, and D. R. Reichman, Elastoplasticity mediates dynamical heterogeneity below the mode coupling temperature, Phys. Rev. Lett. **127**, 048002 (2021).
[30] B. Guiselin, C. Scalliet, and L. Berthier, Microscopic origin of excess wings in relaxation spectra of supercooled liquids, Nat. Phys. **18**, 468 (2022).
[31] Y. Nishikawa, A. Ikeda, and L. Berthier, Collective dynamics in a glass-former with Mari–Kurchan interactions, J. Chem. Phys. **156**, 244503 (2022).
[32] C. Scalliet, B. Guiselin, and L. Berthier, Thirty milliseconds in the life of a supercooled liquid, Phys. Rev. X **12**, 041028 (2022).
[33] M. Vogel and S. C. Glotzer, Spatially heterogeneous dynamics and dynamic facilitation in a model of viscous silica, Phys. Rev. Lett. **92**, 255901 (2004).
[34] P. Charbonneau and G. Tarjus, Decorrelation of the static and dynamic length scales in hard-sphere glass formers, Phys. Rev. E **87**, 042305 (2013).
[35] M. Wyart and M. E. Cates, Does a growing static length scale control the glass transition?, Phys. Rev. Lett. **119**, 195501 (2017), 1705.06588.
[36] X. Xia and P. G. Wolynes, Microscopic theory of heterogeneity and nonexponential relaxations in supercooled liquids, Phys. Rev. Lett. **86**, 5526 (2001).
[37] L. Berthier, G. Biroli, J.-P. Bouchaud, and G. Tarjus, Can the glass transition be explained without a growing static length scale?, J. Chem. Phys. **150**, 094501 (2019).
[38] G. H. Fredrickson and H. C. Andersen, Kinetic Ising model of the glass transition, Phys. Rev. Lett. **53**, 1244 (1984).
[39] J. Jäckle and S. Eisinger, A hierarchically constrained kinetic Ising model, Z. Phys. B **84**, 115 (1991).
[40] W. Kob and H. C. Andersen, Kinetic lattice-gas model of cage effects in high-density liquids and a test of mode-coupling theory of the ideal-glass transition, Phys. Rev. E **48**, 4364 (1993).
[41] C. Toninelli, G. Biroli, and D. S. Fisher, Jamming percolation and glass transitions in lattice models, Phys. Rev. Lett. **96**, 035702 (2006).
[42] F. Ritort and P. Sollich, Glassy dynamics of kinetically constrained models, Adv. Phys. **52**, 219 (2003).
[43] J. P. Garrahan, Glassiness through the emergence of effective dynamical constraints in interacting systems, J. Phys. Condens. Matter **14**, 1571 (2002).
[44] R. L. Jack and J. P. Garrahan, Caging and mosaic length scales in plaquette spin models of glasses, J. Chem. Phys. **123**, 164508 (2005).
[45] R. L. Jack and J. P. Garrahan, Phase transition for quenched coupled replicas in a plaquette spin model of glasses, Phys. Rev. Lett. **116**, 055702 (2016).
[46] G. Biroli and M. Mézard, Lattice glass models, Phys. Rev. Lett. **88**, 025501 (2001).
[47] M. P. Ciamarra, M. Tarzia, A. de Candia, and A. Coniglio, Lattice glass model with no tendency to crystallize, Phys. Rev. E **67**, 057105 (2003).
[48] O. Rivoire, G. Biroli, O. C. Martin, and M. Mézard, Glass models on Bethe lattices, Eur. Phys. J. B **37**, 55 (2004).
[49] R. K. Darst, D. R. Reichman, and G. Biroli, Dynamical heterogeneity in lattice glass models, J. Chem. Phys. **132**, 044510 (2010).
[50] L. Foini, G. Semerjian, and F. Zamponi, Quantum Biroli-Mézard model: Glass transition and superfluidity in a quantum lattice glass model, Phys. Rev. B **83**, 094513 (2011).
[51] Y. Nishikawa and K. Hukushima, Lattice glass model in three spatial dimensions, Phys. Rev. Lett. **125**, 065501 (2020).
[52] See Supplemental Material at http://link.aps.org/supplemental/10.1103/PhysRevLett.132.067101 for additional descriptions of the model, detailed methods for calculating the relaxation spectrum $\chi''(\omega)$, and the physical content of the critical coupling field ε_c, which includes Refs. [30,46,50,51,53–55].
[53] L. Berthier, M. Ozawa, and C. Scalliet, Configurational entropy of glass-forming liquids, J. Chem. Phys. **150**, 160902 (2019).
[54] S. Franz and G. Parisi, Phase diagram of coupled glassy systems: A mean-field study, Phys. Rev. Lett. **79**, 2486 (1997).
[55] L. Berthier and D. Coslovich, Novel approach to numerical measurements of the configurational entropy in supercooled liquids, Proc. Natl. Acad. Sci. U.S.A. **111**, 11668 (2014).
[56] L. Berthier and J. P. Garrahan, Numerical study of a fragile three-dimensional kinetically constrained Model, J. Phys. Chem. B **109**, 3578 (2005).
[57] P. Chaudhuri, L. Berthier, and W. Kob, Universal nature of particle displacements close to Glass and Jamming transitions, Phys. Rev. Lett. **99**, 060604 (2007).
[58] L. Berthier and W. Kob, Static point-to-set correlations in glass-forming liquids, Phys. Rev. E **85**, 011102 (2012).
[59] S. Capaccioli, G. Ruocco, and F. Zamponi, Dynamically correlated regions and configurational entropy in supercooled liquids, J. Phys. Chem. B **112**, 10652 (2008).
[60] M. Ozawa, C. Scalliet, A. Ninarello, and L. Berthier, Does the Adam-Gibbs relation hold in simulated supercooled liquids?, J. Chem. Phys. **151**, 084504 (2019).

[61] C. Cammarota, A. Cavagna, G. Gradenigo, T. S. Grigera, and P. Verrocchio, Numerical determination of the exponents controlling the relationship between time, length, and temperature in glass-forming liquids, J. Chem. Phys. **131**, 194901 (2009).

[62] C. K. Mishra, K. Hima Nagamanasa, R. Ganapathy, A. K. Sood, and S. Gokhale, Dynamical facilitation governs glassy dynamics in suspensions of colloidal ellipsoids, Proc. Natl. Acad. Sci. U.S.A. **111**, 15362 (2014).